Quantum Behavior of Water Protons in Protein Hydration Shell

S. E. Pagnotta,[†] F. Bruni,[‡*] R. Senesi,[§] and A. Pietropaolo[¶]

[†]Centro de Fisica des Materiales, Centro Mixto CSIC-UPV/EHU, Donostia-San Sebastian, Spain; [‡]Dipartimento di Fisica "E. Amaldi" and CNISM-CNR, Università degli Studi Rome Tre, Rome, Italy; [§]Dipartimento di Fisica and Centro NAST (Nanoscienze and Nanotecnologie and Strumentazione), Università degli Studi di Rome "Tor Vergata", Rome, Italy; and [¶]Dipartimento di Fisica and CNISM-CNR, Università Milano-Bicocca, Milan, Italy

ABSTRACT Quantum effects on the water proton dynamics over the surface of a hydrated protein are measured by means of broadband dielectric spectroscopy and deep inelastic neutron scattering. Dielectric spectroscopy indicates a reduced energy barrier for a hydrogenated protein sample compared to a deuterated one, along with a large and temperature-dependent isotopic ratio, in good agreement with theoretical studies. Recent deep inelastic neutron scattering data have been reanalyzed, and now show that the momentum distribution of water protons reflects a characteristic delocalization at ambient temperatures. These experimental findings might have far-reaching implications for enzymatic catalysis involving proton transfer processes, as in the case of the lysozyme protein studied in this report.

INTRODUCTION

Enzyme catalysis is the mechanism by which some proteins are able to accelerate chemical reactions by a factor as large as $10^{19} \pm 10^{21}$ (1,2). The biochemical and physical basis of this fascinating problem, despite the wide amount of experimental data and theoretical work accumulated over the past 60 years (3) (see articles in Dutton et al. (4) for recent reviews), is still far from being completely understood. Advances in transition state theory and computer simulations are providing new insights into the mechanisms of enzyme catalysis, as recently reviewed by Garcia-Viloca et al. (5). Indeed, a comprehensive picture is emerging, in which both lowering of the activation free energy and changes in the generalized transmission coefficient can play a role (5). In particular, a major contribution to this mechanism might come from quantum mechanical tunneling, now firmly established for biological electron transfer (6), and frequently observed and theoretically formalized for enzymic H-transfer (7–11). Whatever is the main mechanism for reaction rate enhancement (activation energy change or tunneling), the changes in enzyme structure and vibrational modes are recognized as fundamental in promoting catalysis (5,8,12,13). Computational and experimental studies have clearly shown that the intrinsic plasticity of the protein, i.e., its conformational changes, could either reduce efficiently the free energy barrier between reactants and products of an enzymatic reaction (5,12,13) or increase the tunneling probability between them, by means of a transient compression of the barrier itself (8–11,14). Such protein dynamics is in turn slaved to that of the solvent, as shown, for example, by recent molecular dynamics simulations and Mossbauer and neutron scattering experiments (15–17). By separating the effects of protein potential surface and of solvent mobility on the atomic fluctuations, it has been shown that it is mainly the solvent mobility that determines the magnitude of protein fluctuations, not only at the protein surface but also in the protein core (15). Moreover, quasi elastic neutron scattering experiments on a globular protein sample show a large dynamical transition, clearly induced by water in the hydration shell at about $T = 200$ K (16). In this framework, the study of the dynamics of proteins hydration water could be thus of particular relevance, especially for a system such as lysozyme, in which a percolative transition strictly related to the enzymatic activity (18) is present. Such transition is known to be due to proton displacements along hydrogen-bonded water molecules adsorbed on the protein surface, with ionizable groups as sources of migrating protons (19,20).

DIELECTRIC SPECTROSCOPY EXPERIMENTS

In this work, we report about an experimental study concerning the aforementioned transition, performed by means of dielectric spectroscopy (DS) with isotopic substitution, and deep inelastic neutron scattering (DINS) techniques.

DS is particularly sensitive to the relaxation of dipoles and to the displacement of charges present in the specimen under investigation, and has been applied to a sample of crystallized and highly purified lysozyme powder. The sample pH and hydration h were adjusted to a final value of 7 and 0.26 g/g, respectively, as previously described (21). The deuterated sample was prepared following a similar procedure. The hydration level $h = 0.28$ g/g corresponds to the same number of hydration water molecules as in the hydrogenated sample. It should be noted that, due to the exchange between hydrogenated (H) and deuterated (D), we cannot exclude that the D_2O hydration shell is slightly contaminated by hydrogen, and the effects of this contamination will be discussed in the following. Measurements were performed in the frequency

Submitted August 27, 2008, and accepted for publication October 31, 2008.

*Correspondence: bruni@fis.uniroma3.it

This article is dedicated to Professor Giorgio Careri (1922–2008).

Editor: Feng Gai.

0006-3495/09/03/1939/5 $2.00

doi: 10.1016/j.bpj.2008.10.062

range from 10^{-2} Hz to 10^{7} Hz, using an Alpha Analyzer apparatus (Novocontrol, Hundsangen, Germany)), and in the temperature range from 210 K to 330 K at constant temperature steps. Data analysis, widely described elsewhere (21), was performed fitting the measured complex spectra, taking into account sample permittivity (expressed as a combination of Havriliak-Negami functions and a conductivity term) and electrode polarization effects (22,23). The expression used reads:

$$\varepsilon^*_m(\omega) = -\frac{\sigma_0}{\iota\omega} + \varepsilon_\infty + \sum_{j=1}^{N} \frac{\Delta\varepsilon_j}{\left[1 + \left(\iota\omega\tau_j\right)^{\alpha_j}\right]^{\beta_j}} + A(\iota\omega)^{d-1}, \quad (1)$$

where σ_0 is the conductivity, ε_∞ is the high frequency limit of the permittivity, N is the number of relaxation processes, and $\Delta\varepsilon_j$ and τ_j are the dielectric strength and the relaxation time for the jth contribution, respectively. A and d characterize the polarizability term. The two exponents α and β appearing in the relaxation term provide an empirical generalization of the ideal Debye relaxation characterized by a single relaxation time instead of a more realistic asymmetric distribution centered around the most probable τ.

Typical dielectric spectra of the H and D lysozyme samples are shown in Fig. 1. The dielectric loss visible in the high frequency region of the spectra is known to be due to water-assisted proton displacement over the protein surface

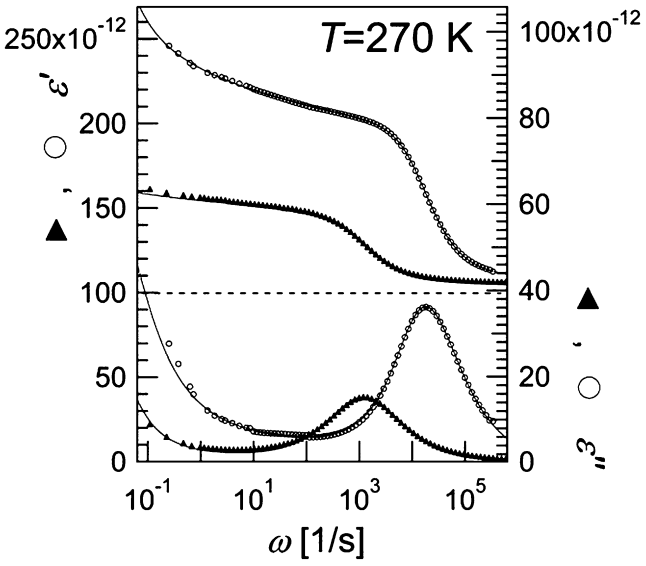

FIGURE 1 Dielectric spectra of hydrogenated (*open symbols*) and deuterated (*solid symbols*) samples at $T = 270$ K, showing a main relaxation at 10^{-3} s^{-1} and at 10^{-4} s^{-1} for the deuterated and hydrogenated samples, respectively. For clarity $\varepsilon'(\omega)$, the real part of the complex permittivity on the right, is arbitrarily shift by a factor of 40, as indicated by the horizontal dashed line. The solid line through the data represents the fit with Eq. 1. Permittivity values are scaled by $\varepsilon_0 S/h$, where ε_0 is the permittivity of vacuum, S is the area of the electrodes of the parallel-plate capacitor, and h is their spacing. Lysozyme samples, from chicken egg white, were purchased from Sigma-Aldrich (St. Louis, MO) and prepared as described in Bruni and Pagnotta (21).

(19,20), and its characteristic frequency (obtained by the fitting procedure and roughly equal to the position of the relaxation peak) gives information on the timescale of such dynamical process. In the fitting procedure, this peak is well resolved in two Havriliak-Negami relaxations: a ''main'' one, describing the proton displacement, and a ''satellite'' one. The nature and temperature dependence of this latter relaxation are discussed in a previous report (21) and will not be considered in this report. It should be noted that although water-assisted, the relaxation time of protons is significantly slower, compared to that of the bound water molecule observable in hydrated proteins around 10^9 s^{-1} at room temperature (24,25). This is due to the fact that with the term ''proton'' here we are actually indicating a ''hydrated proton'' (i.e., H_3O^+); this charged defect forms transiently in one location, the extra H^+ ion being donated by the protein, and it diffuses along the H-bonded network of water molecules adsorbed on the protein surface in a manner similar to the Grotthus mechanism for charge transport in ice. The quite different timescale and the temperature dependence of this latter relaxation compared to that of the water molecules can be thus explained accordingly. As it is clear even from the raw data, the dynamics of the hydration layer in the D-sample appears to be significantly slower than the corresponding one in the H-sample, as indicated by the shift toward low frequencies of the main relaxation peak (Fig. 1). We remark that a contamination of the D-sample due to a small number of protein surface hydrogens will not alter this conclusion, as the observed difference could be only underestimated due to the fast contribution of contaminating hydrogens. This observation, namely the different dynamical behavior of the H- versus the D-sample, becomes more evident considering the relaxation time τ of the main process as a function of the temperature, as shown in Fig. 2. In both H- and D-samples, the dynamics of the system deviates from an Arrhenius behavior and is well described, over the entire range of temperature investigated, by a Vogel-Fulcher-Tamman (VFT) equation:

$$\tau(T) = \tau_0 \exp\left(\frac{B_T}{T - T_0}\right). \quad (2)$$

Such an equation usually describes glassy systems where the dynamics becomes frozen approaching T_0. In particular, in the high temperature limit (or analogously, when $T_0 \rightarrow 0$), the B_T coefficient that appears in Eq. 2 represents an activation energy. Inspection of the VFT parameters (see legend of Fig. 2) shows that the amplitude of the potential barrier B_T for the D-sample is compatible, within the statistical uncertainty, with the energy required to break a hydrogen bond between two adjacent water molecules (~21 kJ/mol) anomalously small for the H-sample (at least in the framework of a ''classical'' transition state theory), even taking into account the difference of ~4 kJ/mol between the zero point energies (26). These observations are in close agreement with the results of a sophisticated theoretical study, using ab initio path integral methodology (27). According to this latter

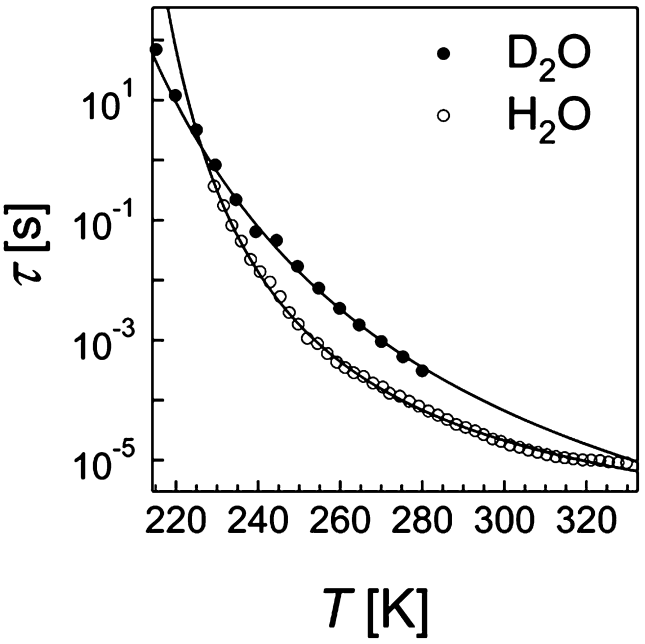

FIGURE 2 Temperature dependence of the relaxation time $\tau(T)$ for the hydrogenated and deuterated samples (*open* and *solid symbols*, respectively). The solid line through the data represents the fit with a VFT equation. For the hydrogenated sample, VFT parameters are $T_0 = 192.9 \pm 0.9$ K, $\tau_0 = (1.33 \pm 0.15) \times 10^{-7}$ s, and $B_T = 4.5 \pm 1.3$ kJ/mol, whereas for the deuterated samples, VFT parameters are $T_0 = 142.4 \pm 2.3$ K, $\tau_0 = (6.3 \pm 6.9) \times 10^{-10}$ s, and $B_T = 15.0 \pm 6.1$ kJ/mol.

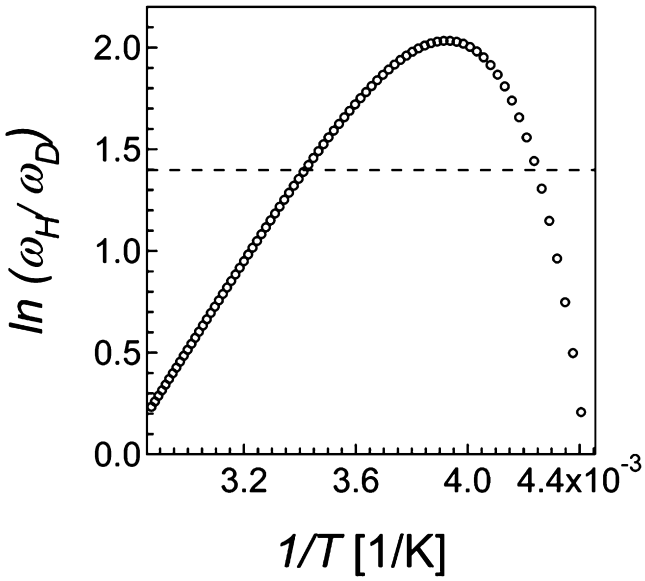

FIGURE 3 Temperature dependence of the isotopic ratio; ω_H and ω_D are the reciprocal of the main relaxation times for H- and D-samples, respectively. The ratio is calculated from the VFT fitting functions shown in Fig. 2. The dashed line represents the ''classical'' expected value of ~1.4.

work, even at 300 K the hydrogen bond energy barrier is reduced from ~15 kJ/mol to ~7 kJ/mol if the quantum nature of the nuclei, along with their motion, is fully taken into account. Scheiner (26) has investigated the effect of interatomic distance on the energy barrier for proton transfer processes in model systems. These quantum mechanical calculations show that the energy barrier for proton transfer increases with the distance between the oxygen atoms of the water. As a result, both the activation energy and the kinetic isotope effect increase. We can evaluate the dielectric analogous of the kinetic isotope effect, here defined as $\tau_D/\tau_H \equiv \omega_H/\omega_D$. In the framework of classical kinetics, such ratio should be temperature independent and roughly equal to the square root of the inverse of the isotope masses ratio. From Fig. 3, however, it is clear that the hydrogen/deuterium displacement over the lysozyme surface cannot be completely described by a classical theory, as it shows a marked temperature dependence, with a maximum at T = 256 K, considerably higher than the expected ''classical'' value of $m_D/m_H \sim 1.4$. The nearly exponential increase with respect to $1/T$ was found by ab initio calculations (28), and confirmed by Bruno and Bialek (10), in the high temperature region investigated by that work. Conversely, the occurrence of the maximum at T = 256 K, along with the decrease of the isotopic effect at low temperatures, suggests the presence of a different mechanism, as quantum effects, and in particular tunneling, play an increasingly larger role as temperature falls. The possible nature of this additional mechanism will be discussed in the concluding remarks of this report. It is of interest to evaluate the average interoxygen distance that would determine the potential barrier B_T as predicted by quantum mechanical calculations cited above (26). In particular, the values found for the amplitude of the potential barrier B_T correspond to a distance of 2.5 and 2.6 Å for the H- and the D-samples, respectively. These distances are both shorter than the average interoxygen distance in bulk water (2.8 Å), indicating that the first hydration shell of lysozyme has a higher density compared to bulk water, in agreement with Merzel and Smith (29), even though the contraction found in this study is not as large as that reported here.

DEEP INELASTIC NEUTRON SCATTERING EXPERIMENTS

The occurrence of quantum phenomena playing a role in the lysozyme hydration shell dynamics, has been recently assessed, although on a quite different time scale, by a DINS experiment (30), performed at the VESUVIO spectrometer at ISIS spallation neutron source. The experiment aimed at the measurement of the momentum distribution of protons, $n(p)$, and mean kinetic energy, $\langle E_k \rangle$, for a lysozyme powder sample prepared as described for DS measurements, at the same pH and hydration level. Two temperatures were chosen, 180 and 290 K, respectively below and above a crossover temperature $T_c = 1.23\, T_g = 269$ K, where $T_g = 219$ K is the glass transition temperature, defined as the temperature where the dielectric relaxation time is 100 s (31). The rationale behind this experiment was to investigate the completely different dynamical regimes for proton displacements on the

hydrated protein below and above T_c. Details on data analysis performed on these samples are reported in Senesi et al. (30). Briefly, the high energy and wave vector transfers achieved in DINS experiments allow describing the scattering process within the framework of the impulse approximations (32,33), where the dynamical structure factor is related to the $m(p)$ through the relation:

$$S_{IA}(\vec{q},\omega) = \int n(\vec{p})\,\delta\left(\omega - \frac{\hbar q^2}{2M} - \frac{\vec{p}\cdot\vec{q}}{M}\right) d\vec{p}. \qquad (3)$$

Here $h\omega$ is the energy transfer, $h^2q^2/2M$ is the recoil energy of the struck atom of mass M, and q is the wave vector transfer. The standard deviation of the $n(p)$, σ, is related to $\langle E_k\rangle$ through the relation: $\sigma^2 = 2M/3h^2\langle E_k\rangle$. The obtained spherically averaged proton momentum distribution, $4\pi p^2 n(p)$, at 290 K showed a narrowing at low p, and a shoulder at high p compared to that measured at 180 K (see Fig. 3 in Senesi et al. (30)), compatible with the transition from a single to a double-well potential. Here we have performed a further step in the data analysis, computing the minimum fraction of protons required to produce the observed difference in the $n(p)$ between the two temperatures. The rationale behind this approach is based on the temperature independence of the proton mean kinetic energies, beside the small kT contribution, as claimed in our previous work (30). These were found to be equal to 215.3 ± 1.5 meV and 216.1 ± 4.4 meV at 180 K and 290 K, respectively (~21 kJ/mol). We have then assumed that the $n(p)$ at 290 K arises from a population of protons with the same $n(p)$ as that at 180 K, plus a contribution due to a fraction of protons showing a characteristic quantomechanical behavior. Therefore, we can write

$$n(p)_{290} = (1-c)n(p)_{180} + cn(p)d, \qquad (4)$$

where c is the fraction of delocalized protons, and $n(p)_d$ is the corresponding momentum distribution.

Fitting the $n(p)$ at 290 K with Eq. 4, we have found that the lower limit of the fraction c, corresponding to a nonnegative $m(p)d$, is $c = 0.29$. Interestingly, this fraction corresponds exactly to the atomic fraction of protons present in the sample and belonging to hydration water. This is of particular importance, because in our DINS experiment we had no way to distinguish between protein and water hydrogens, but this finding strongly indicates that the changes of the proton momentum distribution are indeed due to water hydrogens. We intentionally did not attempt to derive the momentum distribution along particular directions to keep assumptions on the shape of the local proton potential to a minimum. Although the effects of nonsymmetric double-well potential and of transverse momentum distributions would likely give rise to higher concentration, c, our aim is to give a lower bound to this value. Upper and lower bounds to c have been initially estimated by comparing the relative variation of moments (fourth and sixth) of the longitudinal momentum distribution at the two temperatures, i.e., (M_n(290 K) − M_n(180 K))/M_n(290 K), where $M_n(T)$ is the nth central moment at temperature T. These resulted in a lower limit of $c = 0.22 \pm 0.05$ and an upper limit $c = 0.58 \pm 0.12$. Then the fit of Fig. 4 was carried out rejecting all unphysical $n(p)_d$ with negative values (adding a penalty to χ^2 in the fitting program). The resulting value of c is $c = 0.29 \pm 0.01$, as stated above. Importantly, plotting the radial momentum distribution $4\pi p^2 n(p)_d$ (Fig. 4), obtained from the fitting procedure described above (see *inset*, Fig. 4), we notice that this distribution of delocalized protons has a characteristic shape with two well- separated peaks. This is a clear indication of the coherent delocalization of the proton over two sites at a distance r of ~0.6 Å (recall that the relation $p = 2\pi/r$ holds) from the equilibrium position.

CONCLUDING REMARKS

In conclusion, the presence at room temperature of quantum effects in the dynamics of protons over the lysozyme surface, not explainable within a classical picture, is well assessed by both DS and DINS experiment, despite the quite different timescales explored by these two techniques. In particular, DINS gives us indications that, at least on a very short timescale, quantum delocalization plays a fundamental role in shaping the dynamical behavior of protons at ambient temperature. Nevertheless, the decrease of the kinetic isotope effect at low temperatures (Fig. 3), although consistent with the absence of proton delocalization at 180 K (see Fig. 3 of Senesi et al. (30)), strongly suggests the presence of a dynamical

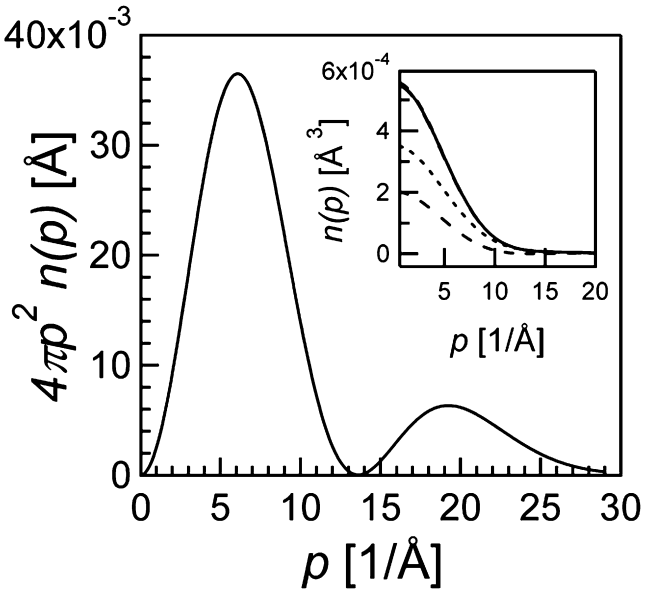

FIGURE 4 Radial momentum distribution of delocalized protons, $4\pi p^2 n(p)_d$, obtained according to the fitting procedure described in the text and defined by Eq. 4. The fraction c of delocalized protons, corresponding to a nonnegative $n(p)_d$, is $c = 0.29 \pm 0.01$. The inset shows the proton momentum distributions $n(p)_{290}$ (*solid line*), $(1-c)\cdot n(p)_{180}$ (*dotted line*) and $c\cdot n(p)_d$ (*dashed line*) as defined in Eq. 4.

arrest at low temperature, as quantum effects play an increasingly larger role as temperature falls. The picture emerging from this study is then compatible with a strong interplay between water and protein dynamics. The protein substrate, directly involved in the establishment of the hydration layer geometry, is indeed not a rigid matrix, but, on the contrary is well known to undergo fluctuations and transitions (34,35) strongly coupled to the dynamics of hydration water (17). Such dynamic fluctuations of the protein molecule could be reasonably considered as responsible for the reduced distance between hydration water oxygens, and thus they are likely to compress transiently the width of the energy barrier experienced by water protons. The dynamical arrest observed for proton displacement below 269 K is therefore directly linked to that of the hydration shell, and in turn to that of the protein. In this context, it is important to notice that the observed deviations from a purely classical behavior of the collective dynamics probed on the millisecond timescale by DS has its origin in the single-particle dynamics probed by DINS, confirming that the dynamical behavior of a hydrated protein is very well described in terms of a proton glass: a system showing dynamical arrest below a crossover temperature, and whose dynamical behavior spans many timescales.

We gratefully acknowledge stimulating discussions with G. Careri, whose seminal work on this subject has been of particular importance for all of us.

REFERENCES

1. Wolfenden, R., and M. J. Snider. 2001. The depth of chemical time and the power of enzyme as catalysts. *Acc. Chem. Res.* 34:938–945.
2. Lad, C., N. H. Williams, and R. Wolfenden. 2003. The rate of hydrolysis of phosphomonoester dianions and the exceptional catalytic proficiencies of protein and inositol phosphatases. *Proc. Natl. Acad. Sci. USA.* 100:5607–5610.
3. Glasstone, S., K. J. Laidler, and H. Eyring. 1941. The Theory of Rate Process. McGraw-Hill, New York.
4. Dutton, P. L., A. W. Munro, N. S. Scrutton, and M. J. Sutcliffe. 2006. *Phil. Trans. R. Soc. B.* 361:1293–1294.
5. Garcia-Viloca, M., J. Gao, M. Karplus, and D. G. Truhlar. 2004. How enzymes work: analysis by modern rate theory and computer simulations. *Science.* 303:186–195.
6. Marcus, R. A., and N. Sutin. 1985. Electron transfer in chemistry and biology. *Biochim. Biophys. Acta.* 811:265–322.
7. Bahnson, B. J., and J. P. Klinman. 1995. Hydrogen tunneling in enzyme catalysis. *Methods Enzymol.* 249:373–397.
8. Sutcliffe, M. J., and N. S. Scrutton. 2000. Enzyme catalysis: over-the-barrier or. through-the- barrier? *Trends Biochem. Sci.* 25:405–408.
9. Masgrau, L., J. Basran, P. Hothi, M. J. Sutcliffe, and N. S. Scrutton. 2004. Hydrogen tunneling in quinoproteins. *Arch. Biochem. Biophys.* 428:41–51.
10. Bruno, W. J., and W. Bialek. 1992. Vibrationally enhanced tunneling as a mechanism for enzymatic hydrogen transfer. *Biophys. J.* 63:689–699.
11. Antoniou, D., and S. D. Schwartz. 1997. Large kinetic isotopic effects in enzymatic proton transfer and the role of substrate oscillation. *Proc. Natl. Acad. Sci. USA.* 94:12360–12365.
12. Eisenmesser, E. Z., D. A. Bosco, M. Akke, and D. Kern. 2002. Enzyme dynamics during catalysis. *Science.* 295:1520–1523.
13. Eisenmesser, E. Z., O. Millet, W. Labeikovsky, D. M. Korzhnev, M. Wolf-Watz, et al. 2005. Intrinsic dynamics of an enzyme underlies catalysis. *Nature.* 438:117–121.
14. Basran, J., M. J. Sutcliff, and N. S. Scrutton. 1999. Enzymatic H-transfer requires vibration-driven extreme tunneling. *Biochemistry.* 38:3218–3222.
15. Vitkup, D., D. Ringe, G. A. Petsko, and M. Karplus. 2000. Solvent mobility and the protein glass transition. *Nat. Struct. Biol.* 7:34–38.
16. Roh, J. H., V. N. Novikov, R. B. Gregory, J. E. Curtis, Z. Chowdhuri, et al. 2005. Onsets of anharmonicity in protein dynamics. *Phys. Rev. Lett.* 95:0381011–0381014.
17. Fenimore, P. W., H. Frauenfelder, B. H. McMahon, and R. D. Young. 2004. Bulk-solvent and hydration-shell fluctuations, similar to - and -fluctuations in glasses, control protein motions and functions. *Proc. Natl. Acad. Sci. USA.* 101:14408–14413.
18. Rupley, J. A., and G. Careri. 1991. Protein hydration and function. *Adv. Protein Chem.* 41:37–172.
19. Pethig, R. 1992. Protein-water interactions determined by dielectric methods. *Annu. Rev. Phys. Chem.* 43:177–205.
20. Careri, G. 1998. Cooperative charge fluctuations by migrating protons in globular proteins. *Prog. Biophys. Mol. Biol.* 70:223–249.
21. Bruni, F., and S. E. Pagnotta. 2004. Dielectric investigation of the temperature dependence of the dynamics of a hydrated protein. *Phys. Chem. Chem. Phys.* 6:1912–1919.
22. Kremer, F., and A. Schnhals. 2002. Broadband Dielectric Spectroscopy. Springer, Berlin.
23. Feldman, Y., R. Nigmatullin, E. Polygalov, and J. Texter. 1998. Fractal-polarization correction in time domain dielectric spectroscopy. *Phys. Rev. E.* 58:7561–7565.
24. Swenson, J., H. Jansson, and R. Bergman. 2006. Relaxation processes in supercooled confined water and implications for protein dynamics. *Phys. Rev. Lett.* 96:247802–247804.
25. Khodadadi, S., S. Pawlus, J. H. Roh, V. Garcia Sakai, E. Mamontov, and A. P. Sokolov. 2008. The origin of the dynamic transition in proteins. *J. Chem. Phys.* 128, 195106(1–5).
26. Scheiner, S., and Z. Latajka. 1987. Kinetics of proton transfer in (H_3CH-CH_3). *J. Phys. Chem.* 91:724–730.
27. Tuckerman, M. E., and D. Marx. 2001. Heavy-atom skeleton quantization and proton tunneling in ''intermediate-barrier'' hydrogen bonds. *Phys. Rev. Lett.* 86:4946–4949.
28. Duan, X., and S. Scheiner. 1992. Energetics, proton transfer rates, and kinetic isotope effects in bent hydrogen bonds. *J. Am. Chem. Soc.* 114:5849–5856.
29. Merzel, F., and J. C. Smith. 2002. Is the first hydration shell of lysozyme of higher. density than bulk water? *Proc. Natl. Acad. Sci. USA.* 99:5378–5383.
30. Senesi, R., A. Pietropaolo, A. Bocedi, S. E. Pagnotta, and F. Bruni. 2007. Proton momentum distribution in a protein hydration shell. *Phys. Rev. Lett.* 98:1381021–1381024.
31. Pagnotta, S. E., R. Gargana, F. Bruni, and A. Bocedi. 2005. Proton momentum distribution in a protein hydration shell. *Phys. Rev. E.* 71:0315061–0315064.
32. Reiter, G., and R. Silver. 1985. Measurement of interionic potentials in solids using deep-inelastic neutron scattering. *Phys. Rev. Lett.* 54:1047–1050.
33. Andreani, C., D. Colognesi, J. Mayers, G. F. Reiter, and R. Senesi. 2005. Measurement of momentum distribution of light atoms and molecules in condensed matter systems using inelastic neutron scattering. *Adv. Phys.* 54:377–469.
34. Wilson, G., L. Hecht, and L. D. Barron. 1997. Evidence for a new cooperative transition in native lysozyme from temperature-dependent Raman optical activity. *J. Phys. Chem. B.* 101:694–698.
35. Daniel, R. M., J. L. Finney, V. Réat, R. Dunn, M. Ferrand, et al. 1999. Enzyme dynamics and activity: timescale dependence of dynamical transitions in glutamate dehydrogenase solution. *Biophys. J.* 77:2184–2190.